High-Resolution Electron Microscopic Investigation of Frustrated Packing of a Semiflexible Liquid Crystalline Polyester

Hee-Tae Jung and Steven D. Hudson*

Department of Macromolecular Science, Case Western Reserve University, Cleveland, Ohio 44106

Robert W. Lenz

Polymer Science and Engineering, The University of Massachusetts at Amherst, Amherst, Massachusetts 01003

Received April 23, 1997; Revised Manuscript Received November 5, 1997[⊗]

ABSTRACT: The structure and morphology of a crystallizable thermotropic main-chain polyester, with a decamethylene flexible spacer, has been investigated by X-ray scattering, electron diffraction (ED), and high-resolution electron microscopy (HREM). Analysis of the electron and X-ray diffraction patterns from quenched specimens suggests a frustrated packing model of smectic order, comprising bundles of chains. This conclusion is supported by HREM imaging of the 17 (002) and 24 Å (011) layer spacings, which confirm two-dimensional ordering. Further insight in the molecular packing is gained by analysis of crystalline structures. Annealing results in one of two different crystal structures, depending on temperature. Low-temperature crystallization is kinetically limited and does not alter the axial packing of the smectic mesophase significantly. Annealing at temperatures near to the nematic phase, however, produces a markedly different crystal structure, which yields a 33 Å (001) reflection. In the latter, more stable phase, the flexible spacers and aromatic mesogens are microphase separated from one another, whereas the former packing represents a frustration of microphase separation and packing strain. Small bundles, of molecules in registry, are shifted axially in the smectic state so as to relax the strain induced by the difference in cross section between the two portions of the molecular repeat unit. Images combining diffraction and phase contrast allow simultaneous visualization of the mesomorphic and semicrystalline phases in annealed specimens. Bright field images of the 33 Å (001) spacing of the high-temperature form enable the crystal size, shape, and relative orientations to be determined. Disclinations have also been examined.

Introduction

Because of their ordered molecular packing, liquid crystalline polymers (LCP's) offer unique mechanical, rheological and optical properties. Although this structure may be characterized by diffraction techniques,[1] certain features of the diffraction from liquid crystals remain controversial, because of the significant disorder inherent in liquid crystalline materials.[2−5] The combination of diffraction and microscopy, however, proves to be a powerful method of structural determination, which is applied here to semiflexible thermotropic polyesters.

Thermotropic polyesters have been of considerable interest scientifically and commercially because of their advantageous balance of mechanical and thermal properties. For application purposes, it is important to control the melting temperature, which can be suppressed in regular rigid molecules using flexible spacers along the main chain or as side substituents.[6,7] In addition to spacer length, the transition temperatures and liquid crystalline phases also depend upon mesogen structure, i.e. number and type of aromatic units, and the placement and orientation of ester linkages.[8−11] For the mesogen derived from terephthalate (T) and hydroquinone (Q) units, which we denote as TQT, containing linear aromatic ester mesogenic units with a polymethylene flexible spacer, Lenz et al. has reported that the stability of the nematic and smectic phases depended on the number of atoms in the flexible spacer.[12] At lower temperatures, these materials are semicrystalline,[13−19] and perhaps because of their easy crystallization, their smectic structure is still in question. Moreover, their smectic ordering may be complex.[1,5,20,21]

Our purpose is to investigate the molecular ordering of the smectic mesophase and the semicrystalline morphologies with different temperature conditions. High-resolution electron microscopy (HREM) has proven to be a powerful tool for structural characterization, and has been performed previously to obtain direct images of a thermotropic smectic liquid crystalline polymer,[22,23] and the effect of smectic order on crystallization was studied.[24] Here, we present the structure and morphology of an aromatic polyester (TQT-10) by using HREM with X-ray and electron diffraction to determine the molecular ordering and the influence of heat treatment. Morphological defects such as the dislocations within, and grain boundaries between, smectic domains are also discussed.

Experimental Section

The material under investigation is a thermotropic polymer with semiflexible coupling chains between the mesogenic units. The synthesis and characterization of this material had been carried out by Lenz et.al.[25,26] The chemical structure of the sample is as follows.

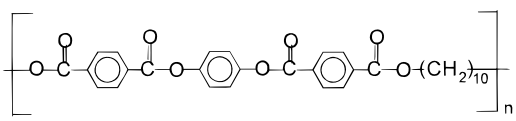

[⊗] Abstract published in *Advance ACS Abstracts,* December 15, 1997.

S0024-9297(97)00549-4 CCC: $15.00
Published on Web 01/23/1998

Figure 1. X-ray diffraction patterns for an oriented fiber of TQT-10H drawn from the nematic melt and annealed at 130 °C. The fiber axis is vertical.

The glass transition, crystal-to-nematic, and nematic-to-isotropic transition temperatures are 67, 231, and 267 °C, respectively, as measured by differential scanning calorimetry and optical microscopy. The molecular weight is estimated to be ~18 000 from intrinsic viscosity measurements. From previous work, this material proved to be well suited for lamellae decoration, though the smectic phase and its morphology were not discussed.

X-ray diffraction from a fiber drawn from the nematic melt was obtained on a Philips system using Ni-filtered Cu Kα radiation before and after annealing at 130 °C for 20 min. The fiber specimen was mounted vertically and perpendicular to the X-ray beam, and diffraction patterns were recorded with a flat film camera at room temperature.

Thin films for electron microscopic investigation were prepared by surface-tension spreading in the nematic melt onto hot phosphoric acid (~240 °C), and quenching as described previously.[16] After transferring the polymer film to a water surface, it was retrieved with Cu screening. To reinforce the film for subsequent thermal treatment, the film was coated with ~200 Å of carbon.

HREM images of the films were obtained at normal incidence with a 100 keV JEOL 100CX TEM by using low-dose procedures appropriate for this type of beam sensitive material, and described in detail by Martin and Thomas.[27] Images and diffraction patterns were recorded at room temperature on Kodak SO-163 electron image film, developed in D-19 developer. The presence and spacing of fringes in the low-dose HREM images were determined with a He/Ne laser optical bench.

Results and Discussion

X-ray diffraction (Figure 1) of a fiber drawn from the nematic melt and then annealed at 130 °C for 20 min shows streaked reflections arranged on or near the meridian on each layer line and strong arced, nearly equatorial diffraction spots that represent crystallinity. Striking features of the WAXS pattern are the strong off-meridian reflection (24Å) on the first layer line and the meridional reflection on the second layer line which gives a layer spacing of 17 Å.

Electron diffraction (ED) patterns, and their schematic representations, after thermal treatment are depicted in Figure 2. The thin films quenched from the nematic melt are indeed highly oriented (Figure 2a). Although the exact nature of the lateral packing can not be precisely defined, it is predominately a disordered smectic phase giving rise to the most intense equatorial. A small amount of microcrystallites may also be present, giving rise to another much less intense reflection, indiscernible at wider angle in Figure 2a. Near the meridian, the strongest reflections occur on the first and second layer lines, and relatively weak reflections are present on the fourth, fifth, and sixth layer lines, consistent with Figure 1. Qualitatively similar patterns from other semiflexible thermotropic LCP's[3−5,20,21] and from low molecular weight liquid crystals[2,28,29] have been analyzed.

Upon annealing the specimen (at 110 or 150 °C), a semicrystalline structure develops: a number of wide angle reflections appear on and near the equator. From analysis of the equatorial spacings, the crystal corresponds to orthorhombic symmetry (i.e. $a \neq b$), as previously determined.[13] However, the meridional and off-meridional reflections are not affected by annealing if the temperature is held less than 180 °C (Figure 2b). These observations suggest that these reflections on or near the meridian do not require crystalline order but instead represent smectic ordering of the liquid crystalline polymer, which is also maintained after crystallization.

In order to determine a possible molecular model of smectic ordering, we examine the localization of scattering intensity (Figure 2a). Note that the (011) reflection on the 1st layer and the (002) reflection on the 2nd layer lines are stronger than the (013), (015), (004), and (006). Strong (011) reflections occur in a cross pattern at 43° with respect to the molecular director, perhaps suggesting that neighboring molecules are shifted axially with respect to one another such that they form layers that are inclined[5] approximately 43° to the direction of molecular orientation (schematically depicted in Figure 3a). Francescangeli et al. recently interpreted their results in such a way, suggesting that the local packing within so-called cybotactic clusters forms small inclined layers.[5] These then are imagined to be embedded in a sea of uniaxial nematic. Such a model is unlikely, however, because the reflections would be streaked and superposed over the first layer line of the nematic. Moreover, in our results the (002) reflection indicates axial ordering and is not consistent with a tilted smectic, which would yield a cross pattern of reflections through the origin (Figure 3a).[30] In a situation in which the first layer line was streaked, a titled layer model suggested that the meridional reflection arises from a high density of stacking faults.[20] However, the following discussion provides a more realistic model for the present case.

Other possible models of different types of regular axial registry between the polymer molecular have been considered. For each model, the structure factors for various reflections were calculated using eq 1,[31]

$$S(hkl) = \sum f \exp(-i2\pi(x_j h + y_j k + z_j l) \qquad (1)$$

where f is the form factor of the molecular repeat unit and x_j, y_j and z_j are the relative positions of other repeat units. This equation allows the relative intensity of various reflections to be calculated, and more significantly, systematic absences to be determined. First, a 2_1 helix, having a pitch of 17 Å and diameter of (~34/tan43° = ~36 Å) would give rise to the pattern of reflections on and near the meridian as obtained. However, these dimensions are not consistent with the

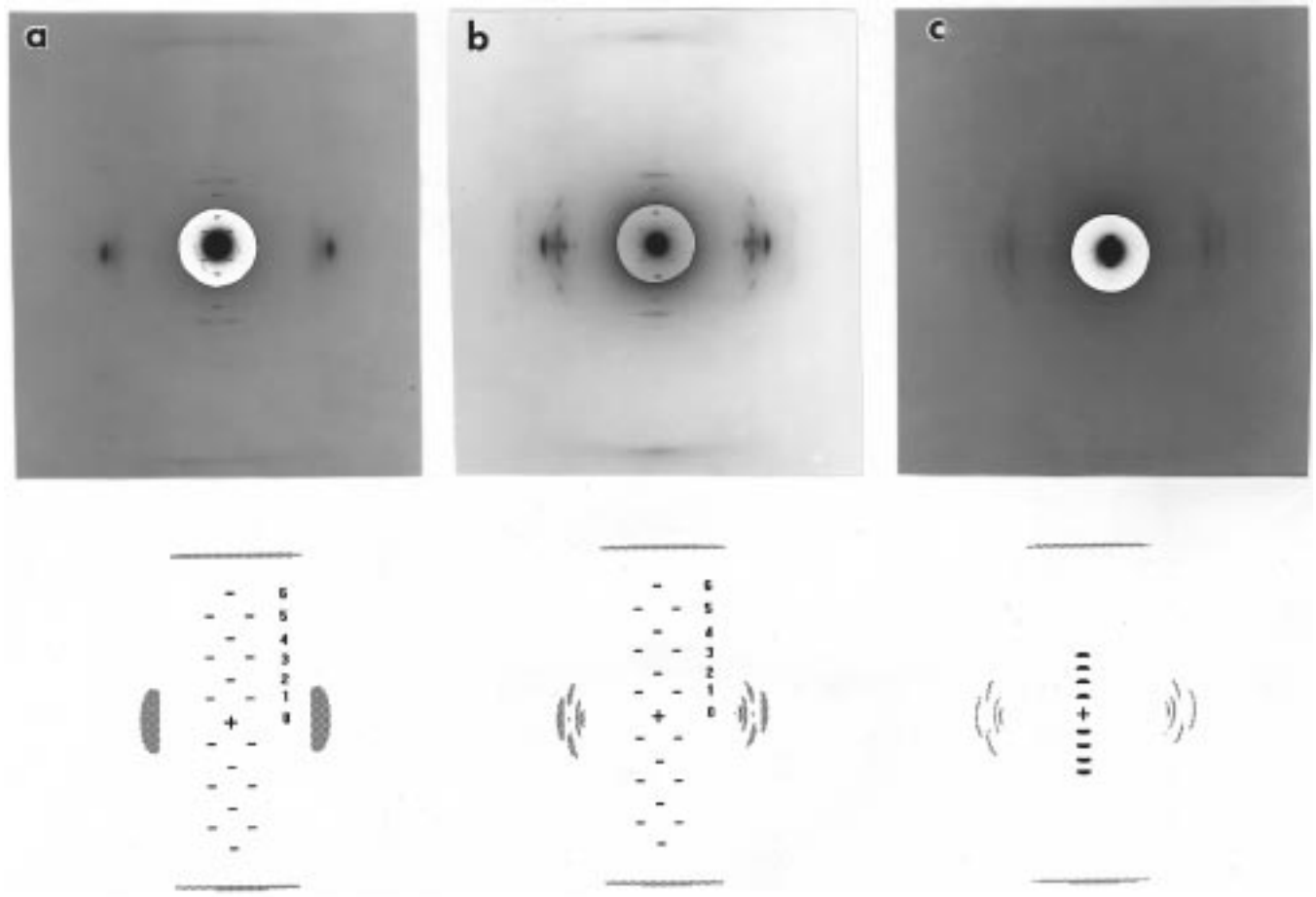

Figure 2. (a) Electron diffraction pattern for an oriented thin film of TQT-10H quenched from the nematic melt (~240 °C) by melt-spreading on H_3PO_4, as described in the Experimental Section. (b) Electron diffraction pattern for a thin film of TQT-10H annealed at 150 °C. (c) Electron diffraction pattern for a thin film of TQT-10H annealed at 215 °C. Differences between the patterns reflect differences in exposure conditions. Likewise, the white circle in the center of each of these patterns represents a reduced exposure, which allows the low-angle reflections to be observed at higher contrast.

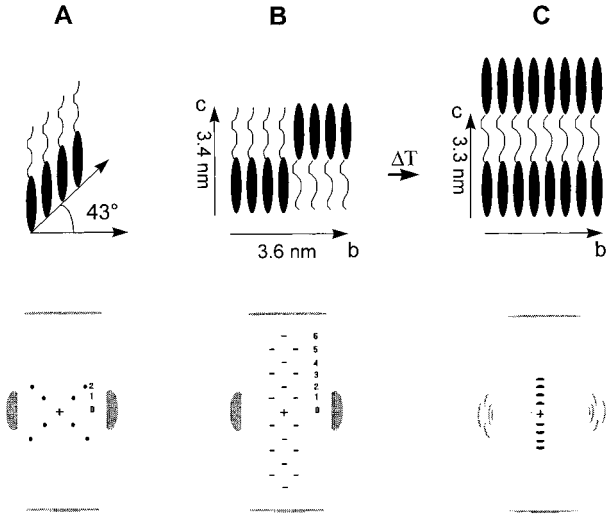

Figure 3. Schematic of the possible molecular layering with annealing temperature. (a) Tilted smectic (not observed). (b) Two-dimensional smectic ordering produced by frustrated molecular registry (observed for annealing temperatures < 180 °C). (c) One-dimensional smectic ordering with complete molecular registry (observed for annealing temperatures ≥ 180 °C).

molecular structure, because the lateral dimension is too large. Furthermore the 2_1 helix model is inconsistent with the high degree of chain alignment that is evident from the wide angle equatorial.

Therefore, smectic packing is proposed. Large lateral dimensions (i.e., 36 Å) may arise if small bundles of chains are packed together. The frustrated packing of Figure 3b comprising bundles of four molecules in registry yields calculation of structure factors that are consistent with the ED data. Registry optimizes favorable molecular interactions (see below), yet extensive packing in registry does not occur, perhaps because of the differing cross-sectional area of the mesogen and spacer. Therefore in order to relieve packing strain, bundles of only four chains (in the *b*-direction) form and the next four are shifted $^1/_2$ of a repeat unit. In this way, competing factors (1) molecular interaction (which favors molecules in registry) and (2) packing strain (which favors molecules shifted) may be optimized. This model is also supported by HRTEM images (Figure 4) which will be discussed later. Small molecular bundles have been proposed recently for the crystalline structure of similar thermotropic polyesters.[32] Interestingly, a "cybotactic nematic" diffraction pattern was also obtained when those fibers were quenched from the nematic melt.[32] Crystallization sharpened the "nematic" reflections and produced meridional reflections that appeared in a similar arrangement to those presented in this work.[32]

Charvolin[33] and Gudkov[34] have discussed examples in which frustrated smectic packing arises from packing strain, though in the latter case, the phenomenon is expressed in terms of "cybotactic blocks of the nematic."

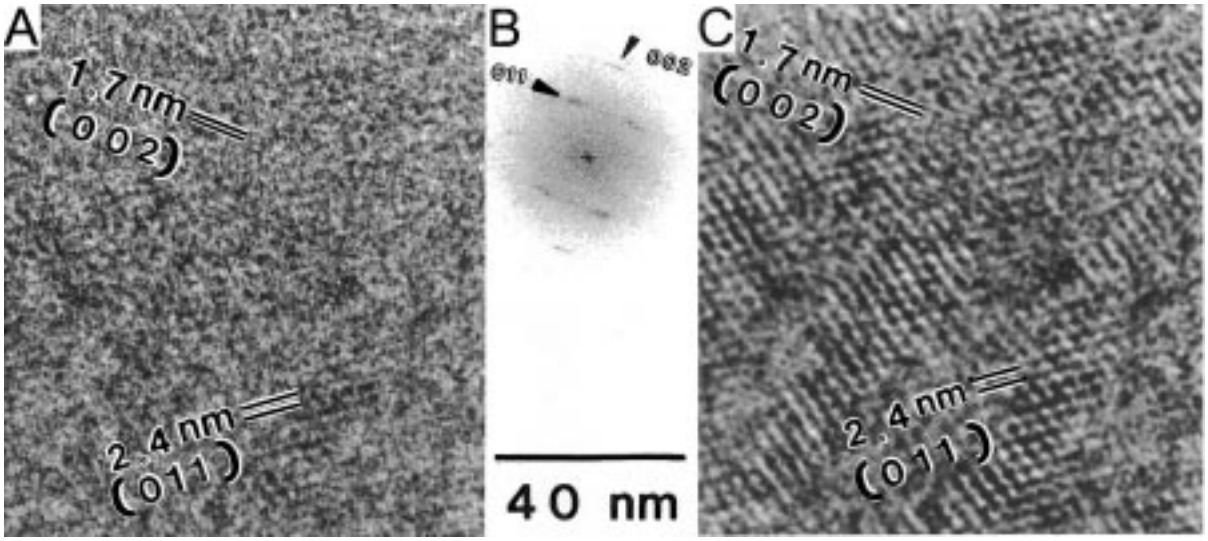

Figure 4. High-resolution electron micrograph (a) and its corresponding power spectrum (b) of a TQT-10H specimen quenched from the nematic melt showing smectic lattice fringes (011) and (200) (c) Fourier-filtered reconstructed image. Note that the (011) and ($0\bar{1}1$) fringes are not present everywhere, but the (002) fringes are. Consistent with this difference in coherence length, the (011) peaks in (b) are broader than the (002) peaks.

This latter example concerns *p*-(*n*-nonylhydroxy)benzoic acid in which there is a difference in cross-sectional area between the hydrogen-bonded head groups and the aliphatic tails. Frustrated packing in smectic LCP's has also been proposed recently by Nakata and Watanabe.[21] The chemical structure of their thermotropic polyester differs significantly, so that frustrated packing arises from a different source of competing factors. They found frustrated packing only in those polymers having an odd number of methylene units in the spacers. In the case of odd spacer lengths especially, the mesogens are tilted with respect to the molecular director. Such tilting increases the energetic driving force for registration of chains. Since the driving force for registry also increases as the difference in spacer lengths is increased, they found that the number of chains within each bundle correspondingly increases. Complete registry, however, does not occur, so that the material avoids spontaneous polarization, in analogy with several low molecular weight frustrated smectics.[28,29] In spite of differences concerning the intermolecular forces responsible for such packing, the diffraction pattern near the meridian on the first and second layer lines is always analogous to Figure 2a and is consistent with general arguments considering the symmetry of a model free energy functional.[29]

A transition occurs at higher annealing temperature (see ED pattern of Figure 2c), resulting in a change in the basic molecular packing. In addition, we find that the higher temperature form is the most stable crystal and can be produced by annealing either the quenched smectic or the lower temperature semicrystalline state. On the other hand, if the high temperature form is annealed at a lower temperature (e.g. 150 °C), it does not transform to the frustrated state. Therefore, the frustrated crystals formed at lower temperature are never found to be stable but are produced (by annealing the smectic state at low temperatures) only because they are able to be formed more rapidly than the more perfect, unfrustrated crystal.

Similar crystallization behavior has also been observed in the analogous polymer having a methyl substituent on the central aromatic ring of the mesogen. At low annealing temperatures, the near meridional scattering is undisturbed by crystallization, which produces many wide-angle near-equatorial reflections. At high annealing temperatures, however, a triclinic crystal is produced, resulting in a significant change in the near meridional scattering.

In the ED pattern of the high temperature form (Figure 2c), all of the off-axis reflections have converted into meridional reflections. This fact and the relative intensity of such reflections suggest a model, in which all chains are in registry (Figure 3c). In the lower-temperature frustrated form, the second layer line reflection (002) is more intense than that on the first layer (011), because the specimen is essentially uniaxially symmetric about the meridional axis and the intensity of the (011) is reduced by the Lorentz geometrical factor, related to the fact that only a fraction of the domains are oriented so as to satisfy the Bragg condition. This condition is always satisfied (assuming perfect uniaxial orientation) for the (002) reflection. After the material converts to the higher temperature from in which the (001) and the (002) reflections are both on the meridian, there is no difference in their Lorentz factors, and their difference in intensity is related simply to differences in the molecular repeat structure factor, $f(hkl)$, as a function of scattering angle (hkl). The atomic potential is clearly much greater in the aromatic portion of the molecular repeat, so that the first order molecular form factor is greater than the second order. That is, since the mesogens and spacers are segregated, the atomic potential contrast represented by the first layer meridian reflection is much larger, and the (001) is now more intense than the (002). Furthermore, the equatorial reflections have become sharper and separated clearly, indicating a higher degree of crystallinity and greater crystal size. However, the symmetry remains orthorhombic, and the position of the equatorial peaks does not change. The packing within the bundles of the lower temperature crystalline form is the same as that within the more extensive planes of the higher temperature form. Transformation from the frustrated smectic to the stable crystal with molecular registry therefore seems to be

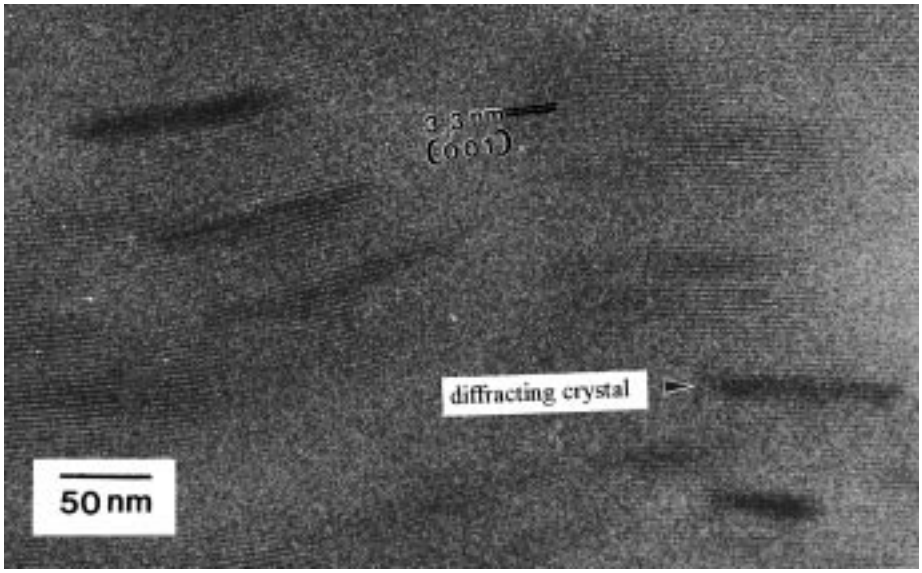

Figure 5. High-resolution electron micrograph of a semicrystalline specimen annealed at 215 °C showing the (001) layer spacing. Diffracting crystalline lamellae appear dark.

accomplished primarily by axial shifting of molecular bundles.

High temperature crystallization is accompanied by a slight expansion of the layer line spacing indicating a slight contraction (from 34 to 33 Å) of the molecule along its axis, which may have been caused by changes in the molecular conformation, especially within the spacer. These local molecular rearrangements are perhaps accompanied by larger scale rearrangements, as suggested by the increased arcing of the meridional reflections; that is, some misorientation between crystallites is expected.

HRTEM. On the basis of the results of X-ray and ED, the conditions for imaging the smectic layers, in particular 24 Å for (011) and 17 Å for (002), could be determined by the phase contrast transfer function. For optimum imaging of smectic planes between 24 and 17 Å, the defocus value ranges from ~0.4 to 0.8 μm. A defocus ~400 nm was used to obtain an image of these planes simultaneously, because the intensity of (002) plane was slightly higher than that of (011) plane on the EM. Figure 4 shows a bright field HRTEM image of a quenched thin film. The smectic layers could be imaged by phase contrast in some regions. In this figure, (011) lattice fringes of 24 Å spacing and (002) fringes of 17 Å spacing are observed directly. The layer spacings were measured from the optical diffraction spectrum to be 24 Å for the (011) lattice and 17 Å for the (002) layer fringe, consistent to previous X-ray and ED result. Clear (011) lattice fringes are observed, inclined ±43° from the molecular axis. Because both (011) fringes superpose one another in several areas of the image, it is not likely that these superpositions correspond to two different overlapping grains but rather that they originate from within the same grain. Therefore, the electron beam must correspond to a zone axis. That is, one set of fringe is (011), the other corresponds to $(0\bar{1}1)$. Since (002) is part of the same zone, these fringes are also seen in the same crystals. The HRTEM image (and optical diffraction pattern) demonstrates two-dimensional ordering and therefore supports the frustrated packing model, as described earlier (Figure 3c). A tilted layer smectic model (Figure 3a) is inconsistent with the high-resolution image because the two first layer−line reflections would represent different domains or grains and would therefore usually produce images in which such fringes do not overlap.

The angle between (002) and (011) lattices is approximately 43°, confirming the ED result from quenched specimens. Although the (002) reflection has a fairly strong intensity in ED patterns, the (002) fringe contrast is lower than that for the (011) fringes. The reason for this may come from differences either in the contrast transfer function or in the relative amplitude of atomic potential corresponding to the two types of fringes. The corresponding power spectrum (Figure 4, inset upper left) shows the (011), (002) reflections. These are arced, indicating lattice distortion in packing the straight stems laterally side by side. Indeed, the direction of lattice fringes is altered from domain to domain, and some of the fringes are curved within a domain. Fourier filtering Figure 4 significantly enhances the contrast of the relatively weak (002) lattice fringes (Figure 4, inset lower left).

For specimens annealed at higher temperature (215 °C) that had transformed to the more stable semicrystalline state, the (001) smectic layer spacing, ~33 Å, could be imaged by phase contrast, using appropriate defocus (Figure 5). The relatively dark, diffuse objects in the image are diffracting lamellar crystals imaged by diffraction contrast, which originated from wide angle reflections being blocked by the objective aperture. These crystals appear diffuse because of the nonzero defocus value. Other crystalline lamellae that do not satisfy the Bragg condition are also present. The average crystal lamellae thickness and lateral crystal size from direct measurement of the image are approximately, 12 (approximately four layers) and 100 nm, respectively, for this annealing condition. The (001) layers are parallel to and extend uninterrupted through a crystal, and their presence within both crystalline and noncrystalline (i.e., smectic) regions indicates that the same axial packing is present in both regions; i.e., the higher temperature annealing produced both a new crystalline and a new smectic-A mesophase (the percent of crystallinity is less than 100%). Like other HRTEM studies of liquid crystalline polymers, during electron irradiation, the lifetime of sharp crystalline reflections

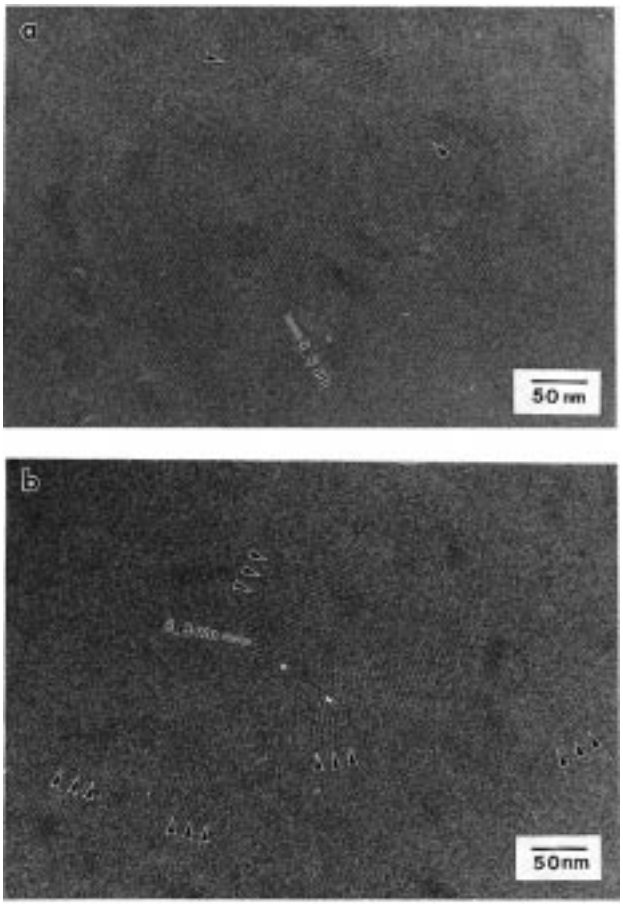

Figure 6. High-resolution electron micrographs of a semicrystalline specimen annealed at 215 °C showing (a) curved layers and (b) a more abrupt reorientation of grains.

on the equator is lower than that of the (001) meridian reflections because the strength of molecular bonding along the chain axis is stronger than the interaction between molecules.[35]

Unlike the (011) fringes of the frustrated semicrystalline state, these (001) fringes are pervasive in the image, so that distortions of the director and disclination defects could be detected. On the basis of diffraction (Figure 2c), the director is oriented perpendicular to the smectic layers. These layers then mark the director orientation much as the crystalline lamellae do, yet at higher resolution. The smectic layers are not straight but are slightly curved and include dislocations (Figures 5 and 6). In other regions, the image is noisy and the layers cannot be discerned, perhaps because of slight deviations of the director (or the specimen film) out of plane.

Other regions of the annealed sample give rise to greater differences in orientation and more numerous defects (Figure 6). In addition to the presence of elementary edge dislocations, an array of edge defects is seen (Figure 6a) to divide the upper right part of the figure, which is misoriented with respect to the rest of the image. Another region of misaligned grains is shown in Figure 6b, in which more abrupt changes of orientation can be seen. Boundaries between grains are not easy to observe because of a high level of noise. The overall orientational pattern of the fringes in Figure 6b suggests that a $s = +1/2$ disclination existed in this neighborhood. Some such misorientation from point to point must have preexisted in quenched specimens, whereas other more abrupt reorientation near boundaries may have been created by relaxation during high-temperature annealing.

Conclusion

The structure and morphology of a semicrystalline thermotropic polyester was investigated. High-resolution electron microscopy (HREM) with X-ray and electron diffraction has been used to obtain information about the smectic structure of the main-chain LCP.

HREM of the quenched smectic provides direct evidence for two-dimensional structure and confirms a frustrated smectic model. The smectic liquid crystalline state comprises bundles of chains that within each bundle, are in registry, and between bundles are shifted axially by a distance equal to half the molecular repeat. This structure represents frustrated packing in which interactions between neighboring molecules are favored by registry, yet strain introduced by such packing is relieved by limiting the bundle size to four chains and staggering the bundles. The proposed model is confirmed by HREM images of superposition of (011) and $(0\bar{1}1)$ lattice fringes. It is not known whether similar bundles exist within the nematic mesophase or not. If so, not only would random shifts exist between bundles but also their size may not be so regular.

The crystal structure that one obtains depends upon the crystallization temperature. Although the more stable form is a uniform registry of chains, crystallization can take place more rapidly from the smectic state, without significant axial displacements. Thus the staggered smectic structure is retained at low annealing temperatures, and the chains order only laterally. At higher annealing temperature, the more stable crystal phase is obtained. As this phase is semicrystalline, HREM and ED indicate that a smectic mesophase without small bundles, and instead, complete registry is simultaneously formed.

Images combining diffraction and phase contrast allow simultaneous visualization of this more highly ordered smectic and semicrystalline phases. The average lamellae thickness and lateral crystal size formed at 215 °C were determined to be, approximately, 12 and 100 nm, respectively. Smectic layers have been imaged in this sample showing evidence of various liquid crystalline defects.

Acknowledgment. We thank ALCOM Grant No. DMR89−20147 for support of this project.

References and Notes

(1) Davidson, P.; Levelut, A. M. *Liq. Cryst.* **1992**, *11*, 469.
(2) deVries, A. *Mol. Cryst. Liq. Cryst.* **1970**, *10*, 219.
(3) Blumstein, A.; Thomas, O.; Asrar, J.; Makris, P.; Clough, S. B.; Blumstein, R. B. *J. Polym. Sci., Polym. Lett. Ed.* **1983**, *22*, 13.
(4) Francescangeli, O.; Albertini, G.; Yang, B.; Angeloni, A. S.; Laus, M.; Chiellini, E.; Galli, G. *J. Polym. Sci., Polym. Phys.* **1995**, *33*, 699.
(5) Francescangeli, O.; Laus, M.; Galli, G. *Phys. Rev. E* **1997**, *55*, 481.
(6) Schmidt, H. W.; Guo, D. *Makromol. Chem.* **1988**, *189*, 2089.
(7) *Recent Advances in Ligand Crystalline Polymers*; Chapoy, L. L. In Chapoy, L. L., Ed.; Elsevier: London, 1985.
(8) Griffin, A. C.; Havens, S. J. *J. Polym. Sci., Polym. Phys. Ed.* **1981**, *19*, 951.
(9) Griffin, A. C.; Britt, T. R. *J. Am. Chem. Soc.* **1981**, *103*, 4957.
(10) Ober, C. K.; Jin, J.-I.; Lenz, R. W. *Adv. Polym. Sci.* **1984**, *59*, 103−146.

(11) Faye, V.; Babeau, A.; Placin, F.; Mauyen, H. T.; Barois, P.; Lanx, V.; Ksaerl, N. *Liq. Cryst.* **1996**, *21*, 485.
(12) Lenz, R. W.; Furukawa, F.; Bhowmik, P.; Garay, R. O.; Majnusz, J. *Faraday Discuss. Chem. Soc.* **1985**, *79*, 229.
(13) Thomas, E. L.; Wood, B. A. *Faraday Discuss. Chem. Soc.* **1985**, *79*, 229−239.
(14) Hudson, S. D.; Thomas, E. L. *Phys. Rev. Lett.* **1989**, *62*, 1993−1996.
(15) Ford, J. R.; Bassett, D. C.; Mitchell, G. R.; Ryan, T. G. *Mol. Cryst. Liq. Cryst.* **1990**, *180B*, 233.
(16) Hudson, S. D.; Thomas, E. L. *Phys. Rev. A* **1991**, *44*, 8128−8140.
(17) Hudson, S. D.; Fleming, J. W.; Gholz, E.; Thomas, E. L. *Macromolecules* **1993**, *26*, 1270−1276.
(18) Ding, D. K.; Thomas, E. L. *Macromolecules* **1993**, *26*, 6531−6535.
(19) Qian, R.; Chen, S.; Song, W. *Macromol. Symp.* **1995**, *96*, 27.
(20) Hudson, S. D.; Lovinger, A. J.; Larson, R. G.; Davis, D. D.; Garay, R. O.; Fujishiro, K. *Macromolecules* **1993**, *26*, 5643−5650.
(21) Nakata, Y.; Watanabe, J. *Polym. J.* **1997**, *29*, 193.
(22) Durst, H.; Voigt-Martin, I. G. *Makromol. Chem. Rapid Commun.* **1986**, *7*, 785−790.
(23) Durst, H.; Voigt-Martin, I. G. *Macromolecules* **1989**, *22*, 168.
(24) Hudson, S. D.; Lovinger, A. J.; Gomez, M. A.; Lorente, J.; Marco, C.; Fatou, J. G. *Macromolecules* **1994**, *27*, 3357−62.
(25) Ober, C.; Jin, J.-I.; Lenz, R. W. *Polym. J.* **1982**, *14*, 9−17.
(26) Zhou, Q.-F.; Lenz, R. W. *J. Polym. Sci., Polym. Chem.* **1983**, *21*, 3313−3320.
(27) Martin, D. C.; Thomas, E. L. *Polymer* **1995**, *36*, 1743.
(28) Sigaud, G.; Hardouin, F.; Achard, M. F.; Levelut, A. M. *J. Phys. (Fr.)* **1981**, *42*, 107.
(29) Prost, J. *Adv. Phys.* **1984**, *33*, 1.
(30) Noel, C.; Navard, P. *Prog. Polym. Sci* **1991**, *16*, 111.
(31) See, for example: Kittel, C. *Introduction to Solid State Physics*, 4th ed.; Wiley: New York, 1971.
(32) Iannelli, P.; Pragliola, S.; Roviello, A.; Sirigu, A. *Macromolecules* **1997**, *30*, 4247.
(33) Charvolin, J. *J. Chim. Phys.* **1983**, *80*, 15.
(34) Gudkov, V. A.; Radzhabova, Z. B. *Ind. Lab. (Engl. Transl.)* **1995**, *61*, 263.
(35) Kumar, S.; Adams, W. W. *Polymer* **1990**, *31*, 15.

MA970549R